Synchronization in dynamical networks: Evolution along commutative graphs

S. Boccaletti,[1] D.-U. Hwang,[1] M. Chavez,[2] A. Amann,[3] J. Kurths,[4] and L. M. Pecora[5]
[1]*CNR- Istituto dei Sistemi Complessi, Largo E. Fermi, 6-50125 Florence, Italy*
[2]*Laboratoire de Neurosciences Cognitives et Imagerie Cérébrale (LENA) CNRS UPR-640, Hôpital de la Salpêtrière, 47 Boulevard de l'Hôpital, 75651 Paris CEDEX 13, France*
[3]*Tyndall National Institute, Lee Maltings, Cork, Ireland*
[4]*Institut für Physik, Universität Potsdam, Am Neuen Palais, PF 601553, D-14415 Potsdam, Germany*
[5]*Code 6362, Naval Research Laboratory, Washington, D.C. 20375, USA*
(Received 5 December 2006; revised manuscript received 18 April 2006; published 5 July 2006)

Starting from an initial wiring of connections, we show that the synchronizability of a network can be significantly improved by evolving the graph along a time dependent connectivity matrix. We consider the case of connectivity matrices that commute at all times, and compare several approaches to engineer the corresponding commutative graphs. In particular, we show that synchronization in a dynamical network can be achieved even in the case in which each individual commutative graphs does not give rise to synchronized behavior.

DOI: 10.1103/PhysRevE.74.016102 PACS number(s): 89.75.Hc, 05.45.Xt, 87.18.Sn

Complex networks, i.e., collections of dynamical nodes connected by a wiring of edges exhibiting complex topological properties, are the prominent candidates to describe the occurrence of collective dynamics in many areas of science [1]. Of particular interest is the existence of synchronized states in such networks. These states indeed are at the basis for the emergence of coherent global behaviors in both normal and abnormal brain functions [2], and play a crucial role in determining the food web dynamics in ecological systems [3].

So far, synchronized behaviors [4] have been mostly studied in the limit of static networks (e.g., networks whose wiring of connections is fixed) with the emphasis focusing on how the complexity in the overall topology influences the propensity of the coupled units to synchronize [5,6]. In particular, it has been established that proper weighting procedures in static complex networks are able to greatly enhance the appearance of synchronized behavior [7].

The very opposite limit of blinking networks [8] has also been considered, where the wiring of connections is rapidly (i.e., with a characteristic time scale much shorter than that of the networked system's dynamics) switching among different configurations. Under these conditions, it has been found that synchronous motion can be established for sufficiently rapid switching times even in the case in which each visited wiring configuration would prevent synchronization under static conditions.

None of these two limits, however, seems an adequate description of many relevant phenomena occurring in natural systems. For instance, properly modeling processes such as *mutation* in biological systems [9], synaptic plasticity in neuronal networks [10], or *adaptation* in social or financial market dynamics [11] would require accounting for time varying networks whose evolution takes place over characteristic time scales that are commensurate with those of the nodes' dynamics.

In this paper, we assess the conditions for the appearance of synchronized states in dynamical networks, *without making any explicit hypothesis* on the time scale responsible for the variation of the coupling wiring. We consider a network of N coupled identical systems, whose evolution is described by

$$\dot{\mathbf{x}}_i = \mathbf{f}(\mathbf{x}_i) - \sigma \sum_{j=1}^{N} G_{ij}(t)\mathbf{h}[\mathbf{x}_j], \quad i = 1, \ldots, N. \tag{1}$$

Here $\mathbf{x} \in \mathbb{R}^m$ is the m-dimensional vector describing the state of the ith node, $\mathbf{f}(\mathbf{x}): \mathbb{R}^m \to \mathbb{R}^m$ governs the local dynamics of the nodes, $\mathbf{h}[\mathbf{x}]: \mathbb{R}^m \to \mathbb{R}^m$ is a vectorial output function, σ is the coupling strength, dots stand for temporal derivatives, and $G_{ij}(t) \in \mathbb{R}$ are the time varying elements of a zero row sum $[\sum_j G_{ij}(t)=0 \ \forall\ i$ and $\forall\ t]$ $N \times N$ symmetric connectivity matrix $G(t)$ with strictly positive diagonal terms $[G_{ii}(t) > 0 \forall\ i$ and $\forall\ t]$ and negative off diagonal terms $[G_{ij}(t) \leqslant 0\ \forall\ i \neq j$ and $\forall\ t]$, specifying the evolution in strength and topology of the underlying connection wiring. Being symmetric $G(t)$ admits at all times a set $\lambda_i(t)$ $[\mathbf{v}_i(t)]$ of real eigenvalues (of associated orthonormal eigenvectors), such that $G(t)\mathbf{v}_i(t) = \lambda_i(t)\mathbf{v}_i(t)$ and $\mathbf{v}_j^T \cdot \mathbf{v}_i = \delta_{ij}$.

It is worth noticing that the zero row sum condition imposed on $G(t)$ can be actually encompassed by a diffusion process when, for instance, the topology of the connectivity matrix reduces to that of a unidimensional chain. In general, a possible way of physically realizing this property is a diffusion process of the output function onto the first neighborhood of a given node (defined as the set of vertices that are adjacent to the node) in the complex topology imposed by the connectivity wiring. Such a condition (and Geršgorin's circle theorem [12]) ensure that (i) the spectrum is entirely semipositive, i.e., $\lambda_i(t) \geqslant 0\ \forall\ i$ and $\forall\ t$; (ii) $\lambda_1(t) \equiv 0$ with associated eigenvector $\mathbf{v}_1(t) = \frac{1}{\sqrt{N}}\{1,1,\ldots,1\}^T$ that entirely defines a synchronization manifold $[\mathbf{x}_i(t) = \mathbf{x}_s(t),\ \forall\ i]$, whose stability will be the object of our study; and (iii) all the other eigenvalues $\lambda_i(t)$ $[i=2,\ldots,N$, $\lambda_i(t) > 0$ for connected graphs$]$ have associated eigenvectors $\mathbf{v}_i(t)$ spanning the transverse manifold of $\mathbf{x}_s(t)$in the $m \times N$-dimensional phase space of Eq. (1).

Let $\delta\mathbf{x}_i(t) = \mathbf{x}_i(t) - \mathbf{x}_s(t) = [\delta x_{i,1}(t), \ldots, \delta x_{i,m}(t)]$ be the deviation of the ith vector state from the synchronization manifold, and consider the $N\times m$ column vectors $\mathbf{X}=(\mathbf{x}_1,\mathbf{x}_2,\ldots,\mathbf{x}_N)^T$ and $\delta\mathbf{X}=(\delta\mathbf{x}_1,\ldots,\delta\mathbf{x}_N)^T$. Then, in linear order of $\delta\mathbf{X}$, one has

$$\delta\dot{\mathbf{X}}=[\mathbb{1}_N\otimes J\mathbf{f}(\mathbf{x}_s)-\sigma G(t)\otimes J\mathbf{h}(\mathbf{x}_s)]\delta\mathbf{X}, \qquad (2)$$

where $\otimes$ stands for the direct product, and J denotes the Jacobian operator. By further considering that the arbitrary state $\delta\mathbf{X}$ can be written as $\delta\mathbf{X}=\sum_{i=1}^{N}\mathbf{v}_i(t)\otimes\eta_i(t)$ $[\eta_i(t)=(\eta_{1,i},\ldots,\eta_{m,i})]$, and applying $\mathbf{v}_j^T$ to the left side of each term in Eq. (2), one finally obtains

$$\frac{d\eta_j}{dt}=\mathbf{K}_j\eta_j-\sum_{i=1}^{N}\mathbf{v}_j^T(t)\frac{d\mathbf{v}_i(t)}{dt}\eta_i, \qquad (3)$$

where $j=1,\ldots,N$ and $\mathbf{K}_j=[J\mathbf{f}(\mathbf{x}_s)-\sigma\lambda_j(t)J\mathbf{h}(\mathbf{x}_s)]$.

The key point is to notice that Eq. (3) transforms into a set of N variational equations of the form $\frac{d\eta_j}{dt}=\mathbf{K}_j\eta_j$, as soon as $\sum_{i=1}^{N}\mathbf{v}_j^T(t)\frac{d\mathbf{v}_i(t)}{dt}\eta_i=0$, i.e., when all eigenvectors are constant in time. This can be realized in two different ways. Namely, either the coupling matrix $G(t)$ is constant (as originally considered in Ref. [6]), or when, starting from an initial wiring condition $G_0=G(t=0)$, *the coupling matrix $G(t)$ commutes at any time with G_0* $[G_0G(t)=G(t)G_0,\ \forall\ t]$. In the following, we will focus on this latter situation, and show that (i) an evolution along commutative graphs can be constructed by starting from any initial wiring G_0 satisfying the set of above mentioned properties, (ii) such an evolution provides a condition for the stability of the synchronous state that can also be fulfilled when the succession of connectivity matrices includes configurations for which the synchronization manifold is transversally unstable, and (iii) the generality of the proposed methods can be illustrated by some typical examples.

Let us now explicitly construct a commutative evolution. We can notice that the initial symmetric coupling matrix can be written as $G_0=V\Lambda V^T$, where $V=\{\mathbf{v}_1,\ldots,\mathbf{v}_N\}$ is an orthogonal matrix whose columns are the eigenvectors of G_0, and $\Lambda_0=\mathrm{diag}[0,\lambda_2(0),\ldots,\lambda_N(0)]$ is the diagonal matrix formed by the eigenvalues of G_0. At any time t, a zero row sum symmetric commuting matrix $G(t)$ can be constructed as

$$G(t)=V\Lambda(t)V^T, \qquad (4)$$

where $\Lambda(t)=\mathrm{diag}[0,\lambda_2(t),\ldots,\lambda_N(t)]$ with $\lambda_i(t)>0\ \forall\ i>1$. The $\lambda_i(t)$ are otherwise arbitrary at this point. With this general form it is easy to show that $G(t)$ is positive semidefinite and since the standard orthogonal basis vectors are not collinear with the eigenvector $\mathbf{v}_1$ we have $G_{ii}>0\ \forall\ i$. Equation (4) therefore gives the formula for generating all possible matrices that commute with $G(0)$, are positive semidefinite with zero row sum, and couple each oscillator in a dissipative fashion ($G_{ii}>0$) to the other oscillators. We refer to this set of matrices as the dissipative commuting set (DCS) of $G(0)$. We note that not all members of the DCS of $G(0)$ are true Lagrangian matrices since it is possible for off-diagonal components to be positive, but all the commuting Lagrangian matrices are contained in the DCS.

Notice that, in particular for $\mathbf{f}(\mathbf{x})=0$ and $\mathbf{h}(\mathbf{x})=\mathbf{x}$ (i.e., in the absence of local dynamics and for an output function that is equal to the identity), Eq. (1) describes a set of coupled homogeneous linear equations. The physical meaning of selecting as coupling matrices the members of the DCS, in this special case, is that the response of the system to external perturbations preserves the same set of eigenmodes.

We could try to constrain the choice of $\lambda_i(t)$ in the generating formula Eq. (4) by, say, writing $\lambda_i(t)=\lambda_i(0)+\delta\lambda_i(t)$ $(i>1)$ and then determining constraints on $\delta\lambda_i(t)$ which would yield only commuting, Lagrangian matrices or coupling matrices for which particular strengths are chosen for particular links. While such constraints can sometimes exist at other times, they result in noncommuting matrices or do not retain a positive, semidefinite form and so are only possible in an approximate way. Generally, this approach is complicated, inexact, and it is difficult to understand the properties of the resulting matrix set. For instance, when $\delta\lambda_k=\delta_{lk}\delta\lambda_l$ $(l\neq 1)$, the elements of $G(t)$ are $G_{ij}(t)=G_{ij}(0)+\delta\lambda_l v_{il}v_{jl}$, so the constraint on the diagonal term reduces to $G_{ii}(t)=G_{ii}(0)+\delta\lambda_l(v_{il})^2\geq 0$ (which is always satisfied for $\delta\lambda_l>0$). This technique allows one to select $\delta\lambda_k=\delta_{lk}\delta\lambda_l$ in order to fix a desired strength $G_{\tilde{i}\tilde{j}}(t)=-d$ $(d\geq 0)$ for the element $\tilde{i}$ and $\tilde{j}$ of $G(t)$ $\left(\delta\lambda_l=-\frac{d+G_{\tilde{i}\tilde{j}}(0)}{v_{\tilde{i}l}v_{\tilde{j}l}}\right)$. Since selection of $\delta\lambda_l$ implies a perturbation to all the other elements $G_{ij}(t)=G_{ij}(0)-[d+G_{\tilde{i}\tilde{j}}(0)]\frac{v_{il}v_{jl}}{v_{\tilde{i}l}v_{\tilde{j}l}}$,one has to select the proper l by minimizing the quantity $\epsilon(l)=\sum_{i,j}^{i\neq\tilde{i}\ j\neq\tilde{j}}\left|\frac{v_{il}v_{jl}}{v_{\tilde{i}l}v_{\tilde{j}l}}\right|$ as a function of l.

In the following we will adopt a more general method which relies on the fact the DCS is the complete set of dissipative, commuting, coupling matrices. Namely, we start from a given initial graph G_0, and produce a large set of different realizations of the same graph. This allows one to calculate the probability distribution $p(\lambda_0)$ of the non null eigenvalues of the set. Then we construct $\Lambda(t)$ in Eq. (4) by randomly drawing a set of $N-1$ eigenvalues $[\lambda_1(t)$ must be always zero$]$ either within the same distribution or using a uniform distribution between $\lambda_2(0)$ and $\lambda_N(0)$. The former strategy can be realized by, e.g., using the spectrum of a different realization of G_0 (henceforth called the eigenvalues surrogate method), or by randomly drawing the eigenvalues of $G(t)$ from the distribution $p(\lambda_0)$ in an ordered $[0<\lambda_2(t),\ldots,\lambda_N(t)]$ or unordered way. The latter strategy can be realized by randomly picking the eigenvalues (in an ordered or unordered way) from a uniform distribution.

It is relevant to study how such procedures modify the main topological structures of the underlying network. In general, $G(t)$ is a dense matrix that can be associated to a symmetric weighted network, whose weight matrix $W(t)$ has elements $W_{ii}(t)=0$, and $W_{ij}(t)=|G_{ij}(t)|$ for $i\neq j$. The main properties of a weighted network are characterized by the average value of the strength distribution, the clustering coefficient, and the average shortest path [1,13]. The distance between two adjacent nodes i and j is given by $l_{ij}=\frac{1}{w_{ij}}$, and the distance along a path $\{n(1),n(2),\ldots,n(m)\}$ can be expressed as $L_{n(1)\to n(m)}=\sum_{k=1}^{m-1}l_{n(k)n(k+1)}$. The shortest path connecting two nonadjacent nodes is then $\ell_{ij}=\min_{\mathrm{allpath}}L_{i\to j}$, and

TABLE I. Statistical properties of the commuting graphs. The table reports average strength $\langle s\rangle = \int sP(s)ds$, the average clustering coefficient $\langle C\rangle$, and the average shortest path length $\langle \ell\rangle$ (see text for definitions and details on the construction of the commuting graphs). In all cases $\langle\dots\rangle$ refers to an ensemble average over 100 different realizations of networks of size $N=500$.

	$\langle s\rangle$	$\langle C\rangle$	$\langle \ell\rangle$
Initial condition G_0 (scale-free)	9.94	5.5773×10^{-4}	5.5144
Eigenvalue surrogate method	11.6881	8.4730×10^{-4}	5.2758
Choosing from $p(\lambda_0)$ (ordered)	12.7042	9.1235×10^{-4}	5.2325
Choosing from $p(\lambda_0)$ (unordered)	142.8746	0.0543	3.7144
Uniform distribution (ordered)	123.6484	0.0634	0.9570
Uniform distribution (unordered)	521.7568	0.6125	1.1098

the network's average shortest path length is $\langle \ell\rangle = \frac{2}{N(N-1)}\Sigma_{i,j}^{i\neq j}\ell_{ij}$[1,13].

As for the clustering coefficient, one can define a clustering of node i as $c_i = \frac{2}{s_i(N-2)}\Sigma_{j,m}W_{ij}W_{im}W_{jm}$, where $s_i=\Sigma_j W_{ij}$ is the strength associated to the node i. The average clustering coefficient $\langle C\rangle$ is then given by $\langle C\rangle = \frac{1}{N}\Sigma_i c_i$, while the strength distribution $P(s)$ characterizes the heterogeneity of the network [13].

Table I reports the results of the mentioned procedures operated on an initial condition G_0 having a power law (scale-free) strength distribution $P(s)\sim s^{-\gamma}$, and taken to be the Laplacian matrix of a scale-free network grown as originally introduced by Barabási and Albert in Ref. [14]. The corresponding strength distributions are plotted in Fig. 1. It is relevant to notice that the eigenvalue surrogate method, as well as the method of choosing the eigenvalues from the initial distribution $p(\lambda_0)$ in an ordered way *do not* change the scale-free behavior of the strength distribution [see the red thick and blue dashed lines in Fig. 1(a)], and provide values for $\langle s\rangle = \int sP(s)ds$, $\langle C\rangle$ and $\langle \ell\rangle$ that *only slightly* deviate from those of the original scale-free network (see Table I). Therefore, both methods provide a convenient way to construct a commuting evolution of the graph (from the scale-free subset of the DCS) that substantially *preserves* all main topological features of the initial condition. At variance, the methods of choosing the eigenvalues from a uniform distribution (either in an ordered or in an unordered) way [red thick solid and blue dashed lines in Fig. 1(b)] completely destroy the original scale-free strength distribution, and provide far different values for each one of the measured quantities. An intermediate situation occurs when choosing the eigenvalue spectrum from the initial $p(\lambda_0)$ in an unordered way. Here, one still preserves the scale-free behavior of the tail [see the black solid line in Fig. 1(b)], but the main topological features of the underlying network are substantially changed from their initial values.

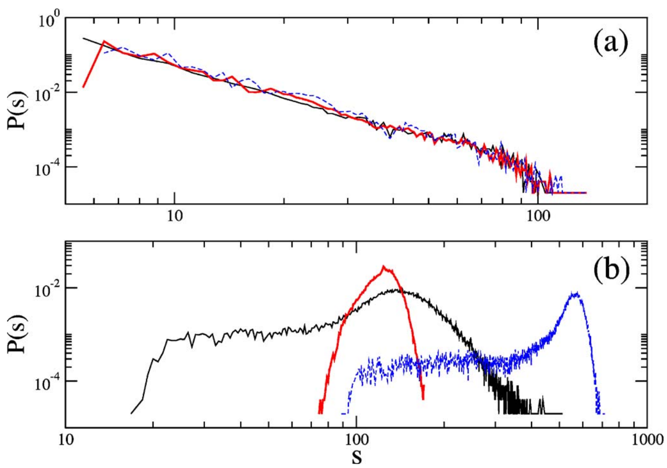

FIG. 1. (Color online) Strength distributions $P(s)$ of the commuting graphs. (a) Initial condition G_0 (black solid line), $G(t)$ constructed by the eigenvalue surrogate method (red thick solid line), and $\Lambda(t)$ obtained by randomly choosing the eigenvalues from $p(\lambda_0)$ in an ordered way (blue dashed line). (b) Eigenvalues randomly chosen from $p(\lambda_0)$ in an unordered way (black solid line), eigenvalues chosen from a uniform distribution in an ordered way (red thick solid line), and in an unordered way (blue dashed line). Other stipulations are as in the caption of Table I.

Notice that both the eigenvalue surrogate method and the method that preserves the distribution $p(\lambda_0)$ in an ordered way basically correspond to construct a network from a spectrum that is statistically equivalent to that of the initial condition G_0. However, any two realizations of a random matrix preserving the probability distribution and the order in the spectrum, in general, *do not* preserve the same eigenvectors, which is, instead, always the case in our procedure. In other words, these methods are a practical way of extracting from the set of all possible realizations of a graph the subset of commuting matrices.

We now discuss the relevant consequences of such a commutative evolution on the stability of the synchronization manifold. Because of the commuting properties of $G(t)$, Eq. (3) becomes $\dot{\eta}_j = \mathbf{K}_j\eta_j$ $(j=2,\dots,N)$. Replacing $\sigma\lambda_j(t)$ by ν in the kernel $\mathbf{K}_j$, the problem of stability of the synchronization manifold is tantamount to study the m-dimensional parametric variational equation $\dot{\eta} = \mathbf{K}_\nu\eta$, with $\mathbf{K}_\nu = [J\mathbf{f}(\mathbf{x}_s) - \nu J\mathbf{h}(\mathbf{x}_s)]$, allowing for graphing the curve of $\Lambda_{\max}$ (the largest of the m associated conditional Lyapunov exponents) vs ν [also called master stability function [6] (MSF)].

When the matrix $G(t)$ is constant, the synchronized state is transversally stable if all λ_i $(i=2,\dots,N)$, multiplied by the same coupling strength σ fall in the range where $\Lambda_{\max}(\nu) < 0$. For a large class of systems, the MSF is negative in a finite parameter interval [6]. This leads to define a key quantity (the eigenratio λ_N/λ_2) that measures the propensity to synchronization of a network and only depends on the topology of the connections. The smaller λ_N/λ_2 is, the more packed the eigenvalues of G are, leading to an enhanced σ interval for which stability is obtained for any choice of $\mathbf{f}(\mathbf{x})$ and $\mathbf{h}(\mathbf{x})$ [6,7].

When $G(t)$ is evolving inside DCS, the eigenvectors are fixed in time, and we can make the hypothesis that at time $T=kdt$, the modulus of each eigenmode η_i $(i\neq 1)$ be bounded by the corresponding maximum conditional Lyapunov exponent $\left(\frac{|\eta_i(T)|}{|\eta_i(0)|}\leq \Pi_{n=0}^{k-1}\exp\{\Lambda_{\max}[\sigma\lambda_i(ndt)]dt\}\right)$. It follows that the condition to be satisfied for transverse stability of the synchronization manifold is that $\forall\ i\neq 1$,

$$S_i = \lim_{T\to\infty}\frac{1}{T}\int_0^T \Lambda_{\max}(\sigma\lambda_i(t'))dt' < 0. \tag{5}$$

Notice that S_i in Eq. (5) is the time average of the maximal transversal (conditional) Lyapunov exponent along the direction of the ith eigenvector (which is fixed in time as far as the connectivity matrix belongs to the DCS set). As so, the integral converges in all those circumstances where all values in time of the maximal transversal Lyapunov exponents in that given direction are finite.

It is worth noticing that Eq. (5) *does not* necessarily imply that $\Lambda_{\max}[\sigma\lambda_i(t)]<0$ at all times. Rather, one can even construct a commutative evolution such that *at each time* there exists one eigenvalue λ_i $[i=i(t)]$ for which $\Lambda_{\max}[\sigma\lambda_i(t)]>0$, and yet obtain a transversally stable synchronization manifold. An example is a periodic evolution with period $T_p=(N-1)\tau$, during which $G(t)$ is given by

$$G(t) = \sum_{l=1}^{N-1} G_l \chi_{[(l-1)\tau,l\tau]}, \tag{6}$$

with $\chi_{[(l-1)\tau,l\tau)}$ being the characteristic function of the interval $[(l-1)\tau,l\tau)$, and the matrices G_l (starting from a given $G_1=V_1\Lambda_1V_1^{-1}$) are constructed as $G_l=V_1\Lambda_lV_1^{-1}$ for $l=2,\ldots,N-1$ with $\Lambda_1=\mathrm{diag}(0,\lambda_2,\ldots,\lambda_N)$, $\Lambda_l=\mathrm{diag}(0,\lambda_{2,l},\ldots,\lambda_{N,l})$, and $\lambda_{j,l}=\lambda_{[\mathrm{mod}_{(N-1)}(j+l-3)]+2}$. If, for instance, $\Lambda_{\max}(\sigma\lambda_2)>0$, then there will always exist a direction in the phase space, along which the synchronization manifold is transversally unstable, but if $\Sigma_{j=2}^{N-1}\Lambda_{\max}(\sigma\lambda_j)<0$, then condition (5) will be satisfied *in all directions* transverse to the synchronization manifold, making it transversally stable.

An example of an extreme situation is illustrated in Fig. 2. Here, an initial scale-free network of $N=200$ Rössler chaotic oscillators is considered, each one of them obeying Eq. (1) with $\mathbf{x}\equiv(x,y,z)$, $\mathbf{f}(\mathbf{x})=[-y-z,x+0.165y,0.2+z(x-10)]$ and $\mathbf{h}[\mathbf{x}]=y$, and the evolution of the wiring follows Eq. (6). For $\sigma=0.03$ we have that $\Sigma_{j=2}^{N-1}\Lambda_{\max}(\sigma\lambda_j)\simeq -9.158$, but $\Lambda_{\max}(\sigma\lambda_j)$ is positive for the first 80 eigenvalues, i.e. *all networks* (if taken as fixed) would make the synchronization manifold unstable in *at least 80 different transverse directions*. Starting from random initial conditions, Fig. 2 reports the temporal evolution of the synchronization error $\langle\delta\rangle(t)=\Sigma_{j=2}^{N}\frac{|x_i-x_1|+|y_i-y_1|+|z_i-z_1|}{3(N-1)}$ at different values of the switching

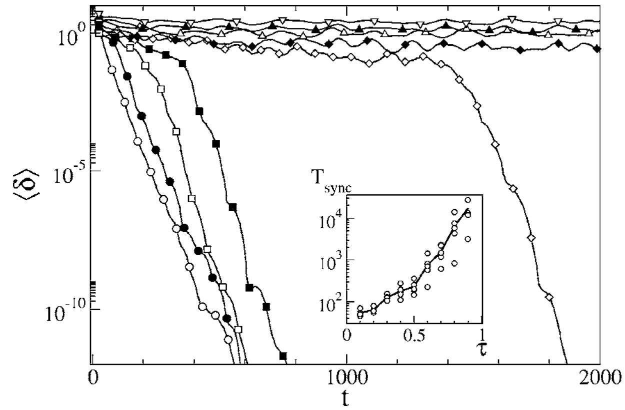

FIG. 2. Time evolution of synchronization error $\langle\delta\rangle$ (see text for definition) for $\tau=0.2$ (empty circles), 0.3 (filled circles), 0.4 (empty squares), 0.5 (filled squares), 0.6 (empty diamonds), 0.7 (filled diamonds), 0.9 (open up triangles), 1.1 (closed up triangles), and 1.5 (open down triangles). In all cases, points refer to an ensemble average over five different random initial conditions for a $N=200$ dynamical network of identical chaotic Rössler oscillators (parameters specified in the text). The inset reports T_{sync} (see text for definition) vs the switching time τ (open circles refer to different initial conditions, solid line graphs the ensemble average).

time τ, showing that the dynamical networked system is indeed able to synchronize, with a transient time T_{sync} to achieve synchronization [the time needed for $\delta(t)$ to become smaller than 0.1, shown in the inset] that scales with τ almost exponentially. While we used this example to illustrate the validity of the synchronization condition (5) under extreme situations, it has to be remarked that neither formula (5) is limited to periodic (or in some other way constrained) evolutions of the connectivity matrices, nor the application of our arguments to extract the general stability conditions of the synchronization manifold is limited to particular choices of the functions $\mathbf{f}(\mathbf{x})$ and $\mathbf{h}(\mathbf{x})$ in Eq. (1).

Furthermore, it must be noticed that different members of the DCS may have vastly different topologies, suggesting that our method is very general and can in principle be applied to a wide set of different situations. Finally, we highlight that the present case is by far different from the fast switching procedure described in Ref. [8]. Indeed, while their case one has to have sufficiently fast switching times among the different network's configuration, here the stability condition *does not* impose in principle any limitation on the switching time τ, making it a plausible representation of the mechanisms at the basis of some natural processes (such as mutation in biological systems or adaptation in social dynamics) that usually involve secular (yet finite) time scales for the evolution of the wiring, and can be thought of as processes that take place to enhance the collective functioning of the network.

The authors are indebted to V. Latora, R. López-Ruiz, and Y. Moreno for the many helpful discussion on the subject. This work was partly supported by projects MIUR-FIRB No. RBNE01CW3M-001 and No. SFB 555 (DFG). S. B. acknowledges the Yeshaya Horowitz Association through the Center for Complexity Science.

[1] R. Albert and A. L. Barabási, Rev. Mod. Phys. **74**, 47 (2002); S. Boccaletti, V. Latora, Y. Moreno, M. Chavez, and D.-U. Hwang, Phys. Rep. **424**, 175 (2006).
[2] F. Varela, J. P. Lachaux, E. Rodriguez, and J. Martinerie, Nat. Rev. Neurosci. **2**, 229 (2001).
[3] E. L. Berlow, Nature (London) **398**, 330 (1999).
[4] S. Boccaletti, J. Kurths, G. Osipov, D. L. Valladares, and C. S. Zhou, Phys. Rep. **366**, 1 (2002).
[5] L. F. Lago-Fernández, R. Huerta, F. Corbacho, and J. A. Sigüenza, Phys. Rev. Lett. **84**, 2758 (2000); T. Nishikawa, A. E. Motter, Y.-C. Lai, and F. C. Hoppensteadt, Phys. Rev. Lett. **91**, 014101 (2003).
[6] L. M. Pecora and T. L. Carroll, Phys. Rev. Lett. **80**, 2109 (1998); M. Barahona and L. M. Pecora, Phys. Rev. Lett. **89**, 054101 (2002).
[7] A. E. Motter, C. S. Zhou, and J. Kurths, Europhys. Lett. **69**, 334 (2005); D.-U. Hwang, M. Chavez, A. Amann, and S. Boccaletti, Phys. Rev. Lett. **94**, 138701 (2005); M. Chavez, D.-U. Hwang, A. Amann, H. G. E. Hentschel, and S. Boccaletti, Phys. Rev. Lett. **94**, 218701 (2005).
[8] I. V. Belykh, V. N. Belykh, and M. Hasler, Physica D **195**, 188 (2004); D. J. Stilwell, E. M. Bollt, and D. G. Roberson, e-print nlin.CD/0502055.
[9] J.-D. J. Han *et al.*, Nature (London) **430**, 38 (2004).
[10] A. Destexhe and E. Marder, Nature (London) **431**, 789 (2004).
[11] P. W. Anderson, K. Arrow, and D. Pines, *The Economy as an Evolving Complex System* (Addison-Wesley, Redwood City, CA, 1988).
[12] S. A. Geršgorin, Izv. Akad. Nauk. SSSR, Ser. Mat. 7, 749 (1931).
[13] V. Latora and M. Marchiori, Phys. Rev. Lett. **87**, 198701 (2001); J. D. Noh and H. Rieger, Phys. Rev. E **66**, 066127 (2002).
[14] A. L. Barabási and R. Albert, Science **286**, 509 (1999).